Pore size matters for potassium channel conductance

David Naranjo,[1] Hans Moldenhauer,[1] Matías Pincuntureo,[1,4] and Ignacio Díaz-Franulic[1,2,3]

[1]Centro Interdisciplinario de Neurociencia de Valparaíso, Universidad de Valparaíso, Playa Ancha, Valparaíso 2360103, Chile
[2]Center for Bioinformatics and Integrative Biology, Universidad Andrés Bello, Santiago 8370146, Chile
[3]Fraunhofer Chile Research, Las Condes 7550296, Chile
[4]Programa de Doctorado en Ciencias, mención Biofísica y Biología Computacional, Universidad de Valparaíso, Valparaíso 2360103, Chile

Ion channels are membrane proteins that mediate efficient ion transport across the hydrophobic core of cell membranes, an unlikely process in their absence. K^+ channels discriminate K^+ over cations with similar radii with extraordinary selectivity and display a wide diversity of ion transport rates, covering differences of two orders of magnitude in unitary conductance. The pore domains of large- and small-conductance K^+ channels share a general architectural design comprising a conserved narrow selectivity filter, which forms intimate interactions with permeant ions, flanked by two wider vestibules toward the internal and external openings. In large-conductance K^+ channels, the inner vestibule is wide, whereas in small-conductance channels it is narrow. Here we raise the idea that the physical dimensions of the hydrophobic internal vestibule limit ion transport in K^+ channels, accounting for their diversity in unitary conductance.

The Journal of General Physiology

Introduction

That the charged nature of K^+ ions impairs their free movement across the plasma membrane derives from elementary physics. The calculation of the Born self-energy for K^+ within the low dielectric constant of the membrane shows the nonspontaneity of this process (Parsegian, 1969). Nevertheless, in K^+ channels, nature found a low-energy mechanism to move K^+ ions across the plasma membrane by developing proteins able to mimic its water coordination (Zhou et al., 2001). Thanks to these membrane proteins, K^+ is the most permeable ion in resting cells, and because K^+ is also the most abundant intracellular ion, the resting membrane potential in most living cells is close to the Nernst potential for K^+ (Hodgkin and Huxley, 1952). K^+ channels are probably an ancient protein family and are present in every living being (Armstrong, 2015). These membrane proteins belong to one of the biggest gene families, with ~90 representatives in the mammalian genome (Yu et al., 2005). Their physiological role is widespread: they guard the resting membrane potential, stabilize osmotic imbalance, set the excitability threshold in excitable membranes, and shape the neuronal action potential (Hille, 2001; Armstrong, 2015).

K^+ channels are endowed with an unsurpassed architectural mechanism that allows K^+ ions to permeate selectively across the cell membrane. However, they show a wide variability in unitary conductance (or ion transport rate), which spans approximately two orders of magnitude when measured under similar experimental conditions. In this viewpoint, we propose that the structural determinants for selectivity and conductance are segregated to two structures within the pore of K^+ channels: the selectivity filter and the internal vestibule, respectively. We raise the idea that the structure of the selectivity filter seems to be so dedicated to selective and efficient K^+ transport that it is unlikely to be the structural determinant of conductance diversity. On the contrary, the physical dimensions of the hydrophobic inner vestibule seem to be the factors that limit K^+ transport, accounting for the difference in unitary conductance among K^+ channels.

The structure of the K^+ permeation pathway

K^+ channels allow selective passage of K^+ ions, thermodynamically lured to flow against their own electrochemical gradient, to the exclusion of all other physiological cations. K^+ channels select for K^+ over Na^+ by almost 1,000-fold, a surprising task considering a difference of <0.5 Å between the ionic radii of these two cations (Hille, 1973). Nevertheless, because the difference in their hydration energies is ~16 kcal/mol, removal of the hydration water should be $\sim 10^{10}$ harder for Na^+ (Robinson and Stokes, 2002). Thus, the simplest explanation for the high K^+ selectivity should involve, at least in part, the need for partial dehydration of the ion, excluding Na^+ because replacing its hydration waters is energetically costlier (Bezanilla and Armstrong, 1972). It has also been argued that the binding sites within the selectivity pore must be precisely shaped around a partially dehydrated K^+ so that it fits snugly (Mullins, 1959). The selectivity sequence of K^+ channels for alkali metal cations ($K^+ \approx Rb^+ > Cs^+ > Na^+ > Li^+$)

Correspondence to David Naranjo: david.naranjo@uv.cl; or Ignacio Díaz-Franulic: ignacio.diaz@cinv.cl

The Rockefeller University Press $30.00
J. Gen. Physiol. 2016 Vol. 148 No. 4 277–291
www.jgp.org/cgi/doi/10.1085/jgp.201611625

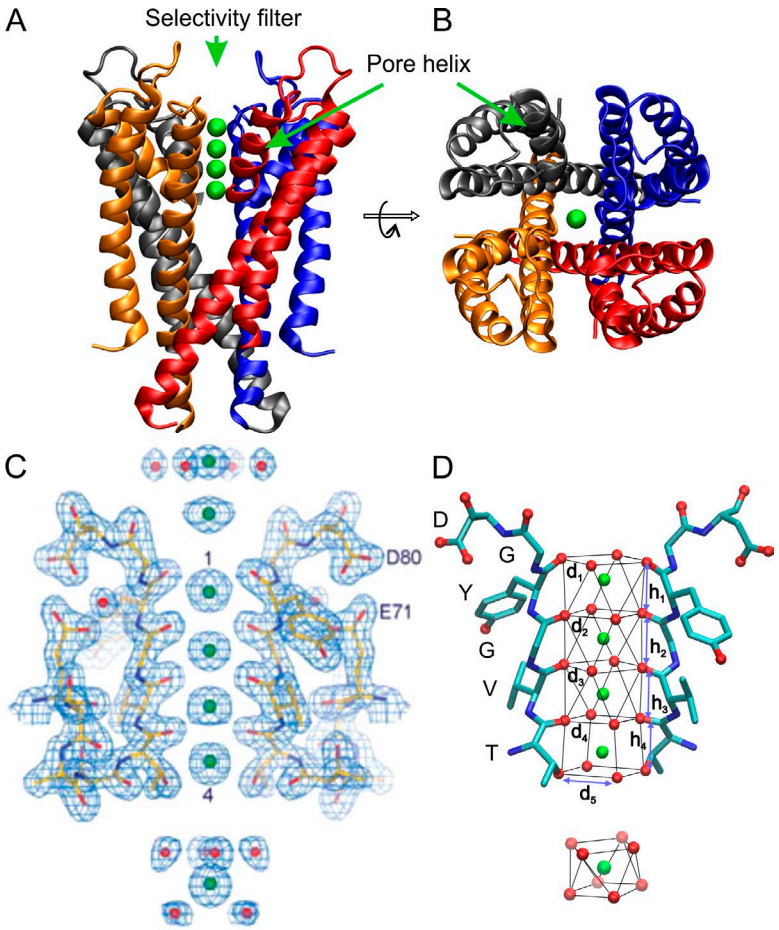

Figure 1. **Structural features of the KcsA channel and K^+ coordination structure in the pore.** (A and B) Membrane-omitted side and top views of the KcsA K^+ channel (PDB ID 1K4C). Each monomer is a two–transmembrane segment peptide position around the pore at the axis of fourfold symmetry forming the K^+ selective pore (green spheres). (C) High-resolution electronic density map showing the two diagonal subunits and the orientation of the carbonyl oxygen atoms to coordinate K^+ ions. The numbers correspond to the four binding sites determined by the sequence TVGYG. (D) Antiprism and cubic cages forming the selectivity filter binding sites, the distances d_1–d_5 and heights h_1–h_4 correspond to the inter-oxygen separations described in Table 1 for several K^+ channel structures. A and B were inspired by Doyle et al. (1998), C was modified from Zhou et al. (2001) with permission from Macmillan Publishers Ltd., and D was inspired by Chen et al. (2014).

indicates that K^+ channel permeation is biased against larger hydration energy and larger size, as expected for a relatively "low-field-strength" site (Eisenman, 1962). Thus, Bezanilla and Armstrong (1972) postulated "Na^+ ions do not enter the narrower part of the pore because they are too small to fit well in the coordination cages provided by the pore as replacements for the water molecules surrounding an ion." Because the observed selectivity sequence is virtually identical among K^+ channels, it anticipates a highly conserved ion selectivity structure (Latorre and Miller, 1983; Heginbotham and MacKinnon, 1993).

The crystallographic structure of the KcsA bacterial K^+ channel resolved at 3.2 Å by Doyle et al. (1998) revealed for the first time how the pore of a K^+ channel looks (Fig. 1, A and B). The protein has a tetrameric organization around the pore placed in its axis of symmetry. Although the structure corresponded to that of a closed channel, it showed several, previously anticipated, functional features: (a) The pore hosts several K^+ ions in single-file order as Hodgkin and Keynes predicted 60 years ago (Hodgkin and Keynes, 1955). (b) The pore has a narrow selectivity filter located toward the external entrance and is flanked internally by a wider internal vestibule as anticipated by Armstrong and Bezanilla (Armstrong, 1971; Bezanilla and Armstrong, 1972; Miller, 1982; Latorre and Miller, 1983). (c) K^+ ions are partially hydrated in the narrow section of the pore, as Mullins, Bezanilla, and Armstrong proposed half a century ago (Mullins, 1959; Armstrong, 1971; Bezanilla and Armstrong, 1972; Hille, 1973). Although the structural analysis could not resolve interatomic bond orientation, it was hypothesized that carbonyl oxygens from the signature sequence in the peptide backbone, TVGYG, shape the anticipated low-field-strength K^+ binding sites by forming surrogate hydration cages in the filter (Eisenman, 1962; Heginbotham et al., 1994). The presence of these expected features in a single crystallographic structure gave this study immediate acceptance.

Later on, crystallization of KcsA channels with improved resolution (2.2 Å) provided a detailed picture of K^+ ions and their carbonyl cages in the selectivity filter (Fig. 1, C and D). At the internal and external entrances, K^+ ions are fully or partially hydrated, whereas those located inside the filter fit perfectly into the four carbonyl-lined binding sites of the selectivity filter (Zhou et al., 2001). Constrained by the K^+/water 1:1 stoichiometry flux ratio, determined from streaming potentials by Alcayaga et al. (1989), it was proposed that

Table 1. **O–O distances at the edges of the water surrogating cages in the selectivity filter, Å**

Selectivity filter edge	Structure (resolution)			
	KcsA 1K4C (2.0 Å)	Kv1.2/2.1 2R9R (2.4 Å)	MthK 4HYO (1.65 Å)	KvAP 1ORQ (3.2 Å)
d_1	3.6	3.5	3.5	4.1
d_2	3.3	3.3	3.2	3.9
d_3	3.3	3.3	3.3	3.9
d_4	3.2	3.3	3.1	3.1
d_5	3.7	3.9	3.6	3.4
h_1	3.1	3.1	3.1	2.9
h_2	3.0	3.0	3.0	2.7
h_3	3.1	3.1	3.2	3.3
h_4	3.0	2.9	2.9	2.9

Center to center inter-oxygen distances at the selectivity filter edges shown in Fig. 1 D. Distance calculations are directly from the Biological Assembly PDB file coordinates. Distances d_i result from the construction of the Biological Assembly. We chose the above structures because they showed the best resolution available at the time.

the four ion-binding sites at the selectivity filter are energetically equivalent for K^+ in alternate occupancy of sites 1–3 and 2–4, with intervening waters at the vacant sites (Bernèche and Roux, 2000; Morais-Cabral et al., 2001). This arrangement makes near to zero the energy cost to put two K^+ ions inside the selectivity filter. In contrast, a solitary K^+ would not be able to permeate measurably because it would be too tightly bound (Neyton and Miller, 1988; Liu and Lockless, 2013). In contrast, double occupancy in sites separated by ∼7 Å (either sites 1 and 3 or 2 and 4) in the selectivity filter affords enough electrostatic repulsion to allow efficient ion translocation along the pore (Åqvist and Luzhkov, 2000; Morais-Cabral et al., 2001).

The geometry of cation coordination in the selectivity filter

The K^+ ions along the selectivity filter are coordinated in a square prism fashion (Fig. 1, C and D), with eight carbonyls groups each contributing a binding site in the selectivity filter, four on top and four below the cation. For sites 1, 2, and 3, the top four carbonyls are rotated ∼45°, forming a squared antiprism with vertices separated by 3–4 Å, whereas a cube encases site 4. Notably, the K^+ located internally to the selectivity filter appears to coordinate eight water molecules also in antiprism fashion, and the most external K^+ is coordinated on top by four waters as if these two cations were caught "in flagrante" getting stripped from their waters before entering the selectivity filter (Miller, 2001; Zhou et al., 2001).

Neutron scattering, spectroscopy, statistical mechanical, and molecular dynamic simulation converge on a mean center to center distance between the K^+ ion and the oxygen atoms of the hydration shell of ∼2.6–2.8 Å (Enderby, 1995; Glezakou et al., 2006; Mancinelli et al., 2007; Bankura et al., 2013). Such a distance matches the center to center separation between K^+ and the carbonyl's oxygen atoms in the selectivity filter.

The mean K^+ coordination geometry in solution is unknown; however, using the above K^+-O separation of 2.6–2.8 Å, it is possible to calculate a vertex to vertex distance of 3.0–3.2 Å in a squared hydration cage. These distances fit well for most of the selectivity filter cages in Table 1. Moreover, a cube, or a squared antiprism, formed by a cage composed of eight water molecules separated by 3.0–3.2 Å would fill a volume of 195–220 $Å^3$, which is the volume of a 3.6–3.8-Å-radius sphere, consistent with the estimated hydrodynamic radius of K^+ (Díaz-Franulic et al., 2015; Moldenhauer et al., 2016). Thus, from the geometrical point of view, the oxygen cages can be regarded as a surrogate water cages. Moreover, this argument favors a homotetrameric structure in K^+ channels as a requisite for highly selective K^+ binding sites, as was proposed by Zhou et al. (2001).

The rigidity of the K^+ selective filter

Electrophysiological, structural, and calorimetry studies support the equilibrium-binding hypothesis for ionic selectivity in K^+ channels: selectivity is attained by making the energy wells along the reaction coordinate deeper for K^+ than for Na^+ (Eisenman, 1962; Neyton and Miller, 1988; Zhou et al., 2001; Piasta et al., 2011; Liu et al., 2012). In light of the conserved structure of the selectivity filter among different channels (Fig. 1, C and D; and Table 1), we are tempted to consider this structure as static and immutable. Nevertheless, functional evidence and intuitive thinking indicate that this temptation is dangerous. Proteins are flexible, and the carbonyl atoms of the selectivity filter fluctuate around 0.4 Å root mean square (Allen et al., 2004), nearly the difference among Na^+ and K^+ ionic radii, suggesting that the snug-fit mechanism requires some amendments (Allen et al., 2004; Noskov et al., 2004). Functionally speaking, selectivity filter flexibility is evidenced in, for instance, C-type inactivation of Kv channels. C-type inactivation is a Na^+-permeable pore conformation in K^+ channel usually triggered by the removal of external K^+ or by long depolarizations (see, for example, Starkus et al. [1997]). This phenomenon has also been seen in the KcsA channel, being associated with the

Table 2. **Single-channel conductance in selected K^+ channels**

Accession no.	Gene	Protein	Pore helix-S6 sequence			pS		Reference
			Pore helix	Selectivity filter	Pore-S6			
Small conductance								
NP_728123.1	*SHAKER*	Shaker	AFWWAVVTMT	TVGYG**D**	MTPVGVWGKIVGSLCAIAGVLTIALPV P VIVSNFNYFYHR	487	20	Carvacho et al., 2008
NP_000208.2	*KCNA1*	Kv1.1	AFWWAVVSMT	TVGYG**D**	MYPVTIGGKIVGSLCAIAGVLTIALPV P VIVSNFNYFYHR	417	10	Gutman et al., 2005
NP_004965.1	*KCNA2*	Kv1.2	AFWWAVVSMT	TVGYG**D**	MVPTTIGGKIVGSLCAIAGVLTIALPV P VIVSNFNYFYHR	419	14	Carvacho et al., 2008
AAC31761.1	*KCNA3*	Kv1.3	AFWWAVVTMT	TVGYG**D**	MHPVTIGGKIVGSLCAIAGVLTIALPV P VIVSNFNYFYHR	737	13	Gutman et al., 2005
NP_002224.1	*KCNA4*	Kv1.4	AFWWAVVTMT	TVGYG**D**	MKPITVGGKIVGSLCAIAGVLTIALPV P VIVSNFNYFYHR	569	5	Gutman et al., 2005
AAA61276.1	*KCNA5*	Kv1.5	AFWWAVVTMT	TVGYG**D**	MRPITVGGKIVGSLCAIAGVLTIALPV P VIVSNFNYFYHR	523	10	Carvacho et al., 2008
NP_002226.1	*KCNA6*	Kv1.6	AFWWAVVTMT	TVGYG**D**	MYPMTVGGKIVGSLCAIAGVLTIALPV P VIVSNFNYFYHR	467	9	Gutman et al., 2005
AAX11186.1	*KCNA7*	Kv1.7	SFWWAVVTMT	TVGYG**D**	MAPVTVGGKIVGSLCAIAGVLTISLPV P VIVSNFSYFYHR	403	21	Carvacho et al., 2008
NP_005540.1	*KCA10*	Kv1.8	GFWWAVVTMT	TVGYG**D**	MCPTTPGGKIVGTLCAIAGVLTIALPV P VIVSNFNYFYHR	466	12	Gutman et al., 2005
NP_004761.2	*KCNB2*	Kv2.2	SFWWATITMT	TVGYG**D**	IYPKTLLGKIVGGLCCIAGVLVIALPI P IIVNNFS**E**FYK**E**	426	15	Carvacho et al., 2008
Large conductance								
P0A334.1	*KCSA*	KcsA	ALWWSV**E**TAT	TVGYG**D**	LYPVTLWGRLVAVVVMVAGITSFGLVT A ALATWFVGR**E**Q**E**	120	100	Nimigean et al., 2003
Q9YDF8.1	*KVAP*	KvAP	ALWWAVVTAT	TVGYG**D**	VVPATPIGKVIGIAVMLTGISALTLLI G TVSNMFQKILVG	253	170	Ruta et al., 2003
O27564.1	*MTHK*	MthK	SLYWTFVTIA	TVGYG**D**	YSPSTPLGMYFTVTLIVLGIGTFAVAV **E** RLL**E**FLINR**E**Q**E**M	104	200	Shi et al., 2011
NP_001240307.1	*KCMA1*	MSlo1	CVYLLMVTMS	TVGYG**D**	VYAKTTLGRLFMVFFILGGLAMFASYV P **E**II**E**LIGNRKKY	332	270	Brelidze et al., 2003

Multiple alignment of the primary structure of K^+ channel pores. The signature sequence TVGYGD on the selectivity filter, used as reference for the alignments, is separated for clarity. Shaker's Gly466 and aligning residues are underlined. Shaker's 475 and aligning residues in Kv channels are individualized for clarity. Aligning with Shaker 475 are KcsA's Ala108, KvAP's Gly241, MthK's Glu92 and MSlo1's Pro320. Aspartates and glutamates are in bold (table modified from Moscoso et al. [2012] with permission from Elsevier).

loss of the second and third selectivity filter K^+ binding sites (Cuello et al., 2010). Selectivity filter stability has been proposed to be important for K^+ discrimination in KcsA, as mutations to surrounding residues (E71; Fig. 1 C) increase Na^+ permeability (Cheng et al., 2011). Thus, a complex network of interactions must support the functional integrity of the selectivity filter. In fact, despite their identical signature sequence and ion distribution along the KcsA and MthK channels selectivity filter, the pore of KcsA, but not MthK, collapses upon K^+ removal (Morais-Cabral et al., 2001; Ye et al., 2010). Thus, the selectivity filter emerges as a dynamic structure, able to adopt a collection of stable conformations, of which the fully conducting ones seem to be also the most often crystallized.

The bacterial nonselective NaK channel, which allows permeation of both K^+ and Na^+, has contributed significantly to our understanding of ionic selectivity in K^+ channels. The NaK channel selectivity filter possesses the sequence TVGDG instead of the canonical TVGYG, failing to show S1 and S2 ion-binding sites (Alam and Jiang, 2009). Variants having the number of binding sites restored to four are K^+ selective, indicating that the ability to make transitions between 1,3 and 2,4 configurations is essential for K^+-selective permeation, revealing a strong marriage between selectivity and conductance (Derebe et al., 2011; Liu and Lockless, 2013; Sauer et al., 2013). Excellent reviews covering the mechanisms of ion selectivity in rich detail are available (Noskov and Roux, 2006; Nimigean and Allen, 2011; Lockless, 2015).

We excluded the inward rectifier family from consideration in this review. Although these channels share with BK and Kvs the selectivity filter and the internal vestibule structures, unlike the latter, their tetramerization domain contributes significantly to ion conduction, adding several K^+-binding sites in series with the pore. Their conduction mechanism looks more complex, and their structural determinants for unitary conductance may be different from Kv and BK channels (Nishida and MacKinnon, 2002; Lu, 2004).

Pore architecture of K^+ channels: Implications for ion permeation

Selectivity filters among different K^+ channels are so similar that we hypothesized that, regardless of their specific unitary conductance, they should be equally competent to allow permeation of K^+ at high rates. However, different K^+ channels display large differences in their unitary conductance measured under similar experimental conditions. Permeation should occur at very high rates because the energy cost of putting two K^+ ions in the selectivity filter is to zero (Åqvist and Luzhkov, 2000; Morais-Cabral et al., 2001; Zhou et al., 2001; Bernèche and Roux, 2003; Allen et al., 2004; Jensen et al., 2013). Accordingly, in standard recording solutions, the selectivity filter accounts for, at most, 3 GΩ (333 pS) of the total pore resistance in both small- and large-conductance K^+ channels (Díaz-Franulic et al., 2015). Direct estimation of electrical resistance, or electrostatic field calculation along the pore, showed that 3 GΩ accounts for 50–90% of the total resistance of BK or MthK channels (Morais-Cabral et al., 2001; Contreras et al., 2010; Díaz-Franulic et al., 2015). In contrast, in Shaker Kv channels, such resistance accounts for only ∼10% of the total (Díaz-Franulic et al., 2015). Thus, in small-conductance Kv channels, ion transport must be limited in structures that are separate from the selectivity filter (Moscoso et al., 2012). Table 2 com-

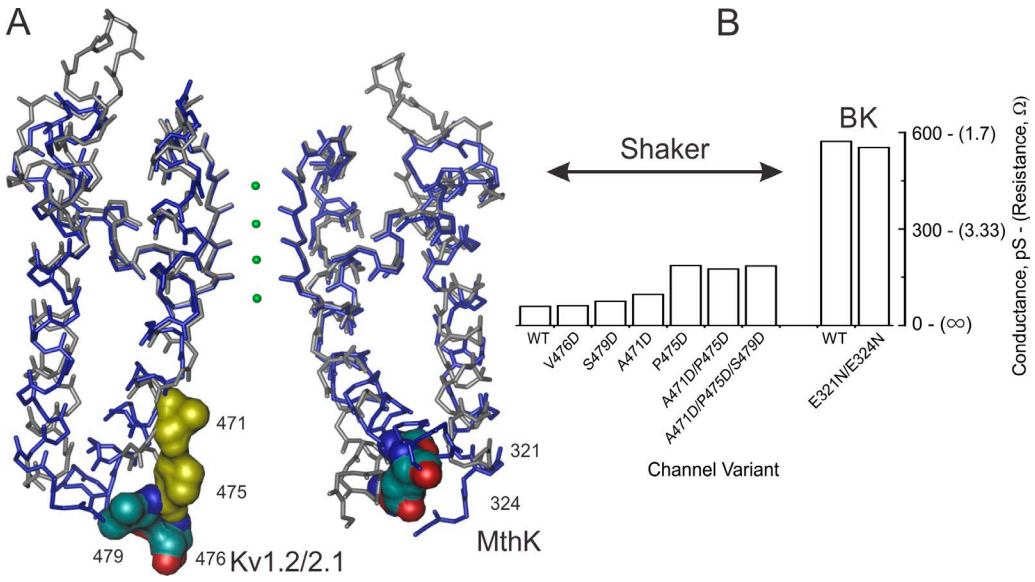

Figure 2. **Occupancy and dimensions of the internal cavity and the maximum conductance of Kv and BK channel.** (A) Alignment of the Kv1.2/2.1 chimera (gray backbone) with MthK (blue) pore domain structures. Shown are the diagonal subunits, with front and back subunits omitted for clarity. K^+/water in the selectivity filter are green spheres. The side chains shown on CPK color correspond to the glutamate ring equivalent positions (right for MthK and left for Kv1.2/2.1). The residues in yellow are the internal cavity residues able to tolerate aspartate substitution. Kv2.1/1.2 chimera: PDB ID 2R9R; MthK: PDB ID 4HYO. (B) Role of charged residues in the inner cavity on maximum conductance of Shaker and BK. Maximal conductance is defined as the unitary conductance at saturating K^+ concentration.

pares the amino acidic sequences of several K^+-selective channels between the pore helix and the C terminus of S6, where the structural determinants for single-channel conductance reside. It is apparent that, although K^+ channels share identical selectivity filter sequences, their unitary conductance ranges from 5 to 270 pS and, accordingly, they fit into two categories: small and large conductance (top and bottom groups in Table 2). Sequence diversity in both groups leads to the idea that the determinants of unitary conductance are located at or near the internal cavity.

Architecture of BK and MthK channels. BK channels (also known as Slo1 or Maxi-K) display the largest unitary conductance among K^+ channels, ranging from ~250 pS under standard recording conditions (100–150 mM K^+) to 600 pS under saturating K^+ concentrations (Eisenman et al., 1986; Brelidze et al., 2003). Sequence analysis of BK channels reveals two conserved glutamate rings (Glu rings) at the internal entrance, comprising Glu321 and Glu324 in each subunit of MSlo (Fig. 2 A). In 100 mM K^+, these eight negatively charged residues double unitary conductance (Brelidze et al., 2003; Zhang et al., 2006). However, such increments vanish at saturating K^+ concentration, indicating that the charged rings contribute to channel conductance by attracting cations and are not an essential part of the efficient K^+ transport mechanism (Fig. 2 B). Therefore, maximum conductance, measured at saturating K^+ concentrations, is required to separate permeation from binding (Díaz-Franulic et al., 2015; Sack and Tilley, 2015). In contrast, Phe380, located at the inner cavity of HSlo (F315 in MSlo), was shown to be critical for ion permeation when replacement with isoleucine or tyrosine decreased unitary conductance by ~70% or ~50%, respectively (Carrasquel-Ursulaez et al., 2015). However, the impact of these mutations on the maximum conductance is unknown.

The internal entrance of BK channels seems wider than in Kv channels. The association rate of internally applied quaternary ammonium to the pore is higher than for Kv channels (Li and Aldrich, 2004; Wilkens and Aldrich, 2006). Also, overlapping dual cysteine modification in BK channels revealed an inner vestibule wider than that of Kv channels (Zhou et al., 2011). Thus, a wide, and possibly short, vestibule could afford a low-resistance pathway for ion permeation in BK channels. This suggests that the dimension of the internal pore entrance limits ionic conduction, such that the presence of large side chain amino acids at the inner entrance reduce BK's unitary conductance, whereas smaller side chain substitutions have little effect (Geng et al., 2011).

In the absence of crystallographic data of BK in the open conformation, the bacterial calcium activated MthK K^+ channel has been validated as a bona fide structural model for the pore domain of BK channels (Geng et al., 2011; Shi et al., 2011; Posson et al., 2013; Moldenhauer et al., 2016). MthK is a large-conductance two–transmembrane segment (TM) channel coupled to a calcium gating ring similar to that of BK (Jiang et

al., 2002; Yuan et al., 2011). Consistent with BK's guessed internal pore dimensions, the MthK structure displays a wide ∼15-Å internal entrance (Fig. 2 A), lined with hydrophobic residues (Table 2).

A direct functional assessment of BK's pore architecture came from Magleby's laboratory with measurements of the "radius of capture" (Brelidze and Magleby, 2005). If the pore is assumed to be a hemispheric sink into which approaching ions vanish, it is possible to use diffusional collisions theory to infer the dimension of the pore entrance in a condition where the rate-limiting step for ion transport is the diffusion of K^+ ions into the entrance of the pore (Läuger, 1976; Andersen, 1983). Assuming K^+ is a rigid sphere approaching the mouth of the channel, the radius of capture corresponds to the difference between the radius of the ion and the radius of the pore entrance (Ferry, 1936; Läuger, 1976) as

$$r_P = r_C + r_i, \quad (1)$$

where r_P, r_C, and r_i are the pore, the capture, and the ion radii, respectively. If the ion is a point charge (r_i = 0), the radius of capture is the same as the radius of the pore. Experimentally, increasing the viscosity of the solution through the addition of high concentrations of sugar, the amplitude of K^+ current becomes asymptotically voltage independent, revealing the limiting K^+ diffusional access to the pore (Läuger, 1976; Brelidze and Magleby, 2005; Díaz-Franulic et al., 2015). In BK channels, the internal r_C is 2.2 Å, a surprising, and debated, number suggesting that the pore is barely wide enough to fit a hydrated K^+ ion (Brelidze and Magleby, 2005). Furthermore, we must consider the hydrodynamic dimensions of K^+ to calculate the pore radius, but the size of hydrated K^+ is not well defined because hydrating water molecules bind with dissimilar energies and lifetimes, forming a fuzzy arrangement. Then, one has to decide how many hydration shells should be added to the radius of the ion. The simplest assumption is to add just one water layer, but this seems arbitrary (Brelidze and Magleby, 2005).

Let's consider that r_P, the pore radius (a functional estimate arising from the radius of capture), is equivalent to the "effective pore radius" (r_E; a structural estimate defined as the radius of the largest sphere that is able to enter the pore cavity; Ferry, 1936). r_E is very easy to estimate from the wealth of K^+ channel structures available, and for MthK it is 5.7–5.9 Å (Moldenhauer et al., 2016). Thus, by replacing r_E for r_P in Eq. 1, we obtain r_i = 3.5–3.7 Å for K^+. These figures are consistent with K^+ ions carrying only one hydration layer (Enderby, 1995; Glezakou et al., 2006; Mancinelli et al., 2007; Bankura et al., 2013). Bearing in mind that the radius of capture is measured at room temperature, in liquid phase, and with operative friction forces, the harmonious outcome with structural studies, made at very low temperature, in solid phase, and in equilibrium, is satisfying.

Architecture of Shaker and Kv channels. We have seen that side chain volume and charge of residues at the internal entrance of large-conductance channels restrict K^+ conductance (Brelidze et al., 2003; Nimigean et al., 2003; Geng et al., 2011). Thus, K^+ channels having narrower pores should display smaller unitary conductance. Among the small-conductance K^+ channels the most extensively studied is the *Drosophila melanogaster* Shaker K^+ channel. As expected, Shaker ionic selectivity is lost upon mutation of some of the selectivity filter residues (Heginbotham et al., 1994). Shaker's unitary conductance ranges from ∼20 pS in ∼100 mM K^+ to 60 pS in saturating 3,000 mM K^+ (Heginbotham and MacKinnon, 1993; Díaz-Franulic et al., 2015). Intra- and intersubunit metal coordination at the internal entrance suggests that this region is narrower than that in BK or MthK and/or that the opening conformational change implies a small physical displacement (Webster et al., 2004; del Camino et al., 2005). Consistent with a narrow pore, the crystal structure of Kv1.2, a mammalian homologue of Shaker, shows an internal entrance of ∼10 Å, which, as occurs in MthK, is lined with hydrophobic side chains (Long et al., 2005a, 2007). Thus, the narrow Kv internal cavity is just large enough to let ions go across, and "…may help to explain why Shaker has an approximately tenfold lower conductance than its bacterial relatives" (Webster et al., 2004).

As with BK, measurements of diffusion limited outward currents allowed us to estimate that Shaker's cytosolic radius of capture was ∼0.8 Å, ∼1.4 Å narrower than BK's (Díaz-Franulic et al., 2015). As seen with MthK/BK in section Architecture of BK and MthK channels, this estimate of r_C is consistent with the effective opening of the open Kv1.2/2.1 chimera if we assume that the hydrodynamic radius for K^+ is ∼3.5–4.4 Å (Díaz-Franulic et al., 2015; Moldenhauer et al., 2016). As hypothesized, such a narrow cavity contributes decisively to the total electrical resistance of the pore. Estimations of the sectional resistance along the pore of Shaker showed that, in contrast to BK, the inner cavity entails an electrical resistance ∼55–fold larger (or 1/55 lower conductance) than that of BK channels (Díaz-Franulic et al., 2015). Thus, these results reinforce the idea that the size of the internal vestibule severely limits single-channel conductance of small-conductance K^+ channels.

The internal pore dimensions and K^+ channels cytosolic structure. For both Kv and MthK structures, the effective entrance is consistent with the estimates of the radius of capture of Shaker and BK channels, respectively, when the K^+ hydrodynamic radius is taken as ∼4 Å (Díaz-Franulic et al., 2015; Moldenhauer et al., 2016). However, the canonical Kv channel activation bundle

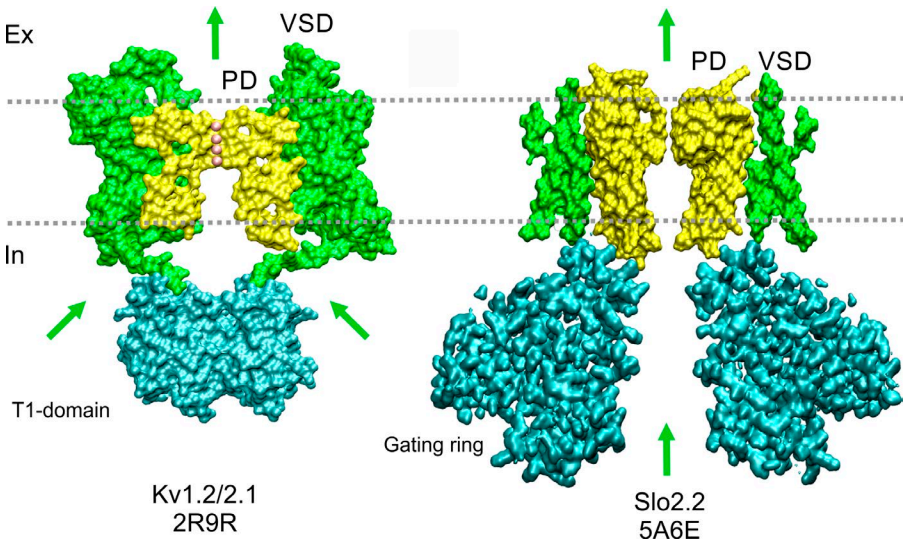

Figure 3. **K^+ channel structural topology.** Surface representation of Kv (Kv1.2/2.1 chimera; left) and BK (Slo2.2; right) structures. Green and yellow colors represent the voltage-sensing domain (VSD) and the pore domain (PD), respectively. The green arrows show the putative conduction paths for ions that in Kv channels K^+ access/exit through the lateral windows of the "hanging" T1 domain (the gondola in cyan), whereas in BK the ions cross the entire gating ring formed by the RCK domains (in cyan). The pink spheres are K^+ ions, and the horizontal discontinued lines indicate the approximate inner and outer boundaries of the membrane. External side is up. The Kv figure is a 6-Å slab prepared with VMD, with $-6 < x < 0$ (Humphrey et al., 1996). BK front and rear subunits are removed for clarity (inspired by Hite et al. [2015]).

crossing gate, located at the lower end of S6, appears to be missing in BK channels. Instead, these K channels may gate the ion pathway near the selectivity filter (Wilkens and Aldrich [2006], Garg et al. [2013], and Posson et al. [2013]; but see Hite et al. [2015]). Thus, the estimates of radius of capture could represent the pore dimensions at different depths in the permeation pathway. Because the estimates of the hydrodynamic size of K^+ produced by both comparisons (MthK with BK and Kv1.2 with Shaker) are so similar, the possible discrepancy in deepness should not account for more than 1 Å in radius. In addition, the resulting size of K^+ agrees well with estimations for the hydrated K^+ in aqueous solutions obtained using unrelated techniques (Enderby, 1995; Glezakou et al., 2006; Mancinelli et al., 2007; Bankura et al., 2013).

There is one more problem with the estimation of the internal pore dimension based on the radius of capture for BK and Kv channels. These measurements disregard the contribution of important intracellular domains in both proteins, leading to an oversimplified structural image (Long et al., 2005a; Hite et al., 2015). Both BK and Kv channels have tetramerization domains near the internal entrance (Kobertz and Miller, 1999; Krishnamoorthy et al., 2005; Hite et al., 2015). In Kv channels, the four tetramerization domains (T1) form a structure known as "the hanging gondola" because it hangs from the pore domain through four linkers, leaving four side-facing openings for ion transport (Fig. 3; Kobertz and Miller, 1999; Long et al., 2007). Meanwhile, the structure of Slo2.2, a BK channel, shows the calcium-dependent gating ring forming a funnel structure that could guide ions into the pore cavity (Hite et al., 2015). Both structures project negative electrostatic potential into the permeation pathway, raising local K^+ concentration, but contribute, at most, to 30% to the unitary current (Kobertz and Miller, 1999; Budelli et al., 2013; Hite et al., 2015).

Why does a narrow pore cause larger resistance?

How is it possible that the internal cavity of Kv channels, with a radius only 1.4 Å smaller than that of BK, causes a 55-fold increase in resistance? The seminal paper by Parsegian (1969) predicted that the energy required to put an ion inside an aqueous pore embedded in the low dielectric membrane could decrease by up to 28 kcal/mol for every Å increase in sectional radius. Thus, a mere 1-Å narrower pore would represent a much larger energy barrier for the ion to overcome. Energy calculations show that K^+ transport in the nonpolar nanotube membrane model is highly sensitive to the dimensions of the pore. In narrow pores (<5-Å opening diameter) ion transport cannot occur, but wider pores (~10-Å opening diameter) are highly permeable, with ionic mobilities comparable with those seen in bulk solution (Peter and Hummer, 2005). In contrast, narrow pores would strip off solvation waters, paying a large energetic penalty; in contrast, wider pores would keep the first hydration shell intact. The free energy calculated for K^+ ions inside the cavity of K^+ channels is indeed a few kcal lower in the wider parts of the pore (Chung et al., 2002; Jogini and Roux, 2005; Treptow and Tarek, 2006). Thus, higher resistances may result from the reduced probability of finding an ion inside narrower pores, and, conversely, we expect that decreasing the energy required to put an ion inside the cavity will result in an increased conductance (see section Turning Shaker into a large-conductance K^+ channel below). We have to keep in mind that these considerations involve using equilibrium energies to describe the nonequilibrium phenomenon that is ion transport. Nevertheless, because diffusion and water

turnover are orders of magnitude faster than permeation, an equilibrium approximation should be at least partially satisfactory (Hille, 2001; Grossfield, 2005; Mancinelli et al., 2007).

Because ion conduction occurs away from equilibrium, we should also consider the action of frictional forces on unitary conductance. We are required to acknowledge that ions must interact physically with their surroundings (Eisenberg, 2013). Also, molecular dynamics simulations have shown drastic reductions of ion and water diffusion coefficients inside wide pores (Wilson et al., 2011; Zhu and Hummer, 2012b). As expected for friction, such reduction seems to be caused by the pore shape and wall tortuosities. Because of the lack of room inside the inner vestibule of Kv channels, fully or partially hydrated ions would be bumping into the walls of the pore. In contrast, in BK channels, with a 1.4-Å wider cavity, there is enough room for a loosely attached extra layer of water molecules interfacing with the walls of the inner pore. In principle, these interfacial waters should bear low mobility (because of their low entropy); nevertheless, recent molecular dynamic simulations show highly mobile and chaotic interfacial waters in narrow nanotubes organic-aqueous contact (Garate et al., 2014). Such loosely attached water molecules may lubricate the passage of the K^+ cage, working as ball bearing sliders.

Turning Shaker into a large-conductance K^+ channel

In agreement with the equilibrium energy hypothesis, lowering the K^+ energy inside the cavity is expected to increase unitary conductance, by increasing pore occupancy. Indeed, introducing negatively charged residues at Shaker's internal entrance (position Pro475) increases unitary conductance by eightfold (Sukhareva et al., 2003; Moscoso et al., 2012). Such an increment was correlated with the appearance of a cytosolically accessible K^+ site that could enhance Mg^{2+} blockade by preventing its exit toward the cytosol. Molecular dynamics simulations showed a largely increased K^+ occupancy and Mg^{2+} binding at the inner cavity. Two distal K^+-binding sites flanked Mg^{2+} exit (Moscoso et al., 2012). Because of the deep impact of mutations of Pro475 on channel gating (Hackos et al., 2002), it was quite possible that P475D had enlarged pore size, accounting for such an increased conductance. However, the radius of capture was found to be identical to that of Shaker-WT (Díaz-Franulic et al., 2015). This is in satisfying agreement with the Parsegian hypothesis because it shows that it is possible to raise conductance by several-fold just by increasing pore occupancy, i.e., by lowering the work needed to put an ion in the cavity. Several other charges added to the internal vestibule (471D, 476D, and 479D) also increased unitary conductance; nevertheless, no additional change could increase maximum conductance beyond 200 pS, which is one third of BK's conductance (Díaz-Franulic et al., 2015). Part of the other two thirds of the difference in unitary conductance between Kv and BK channels might have different causes: fluctuations of the selectivity filter or friction. In the former case, differences in the selectivity sequence should be expected (Starkus et al., 1997; Allen et al., 2004; Cheng et al., 2011).

Electromechanical coupling and permeation determinants map to the same hotspot

Voltage-activated K^+ channels are impressive examples of evolutionary functional tuning. On one hand, the addition of several sensing modules to the seemingly permeation-optimized voltage- and calcium-activated BK pore domain gives them the ability to integrate complex stimuli into transmembrane K^+ fluxes. On the other hand, voltage sensitivity of Kv channels seems to be near the maximal possible, limited only by the capacity of the voltage-sensing domain to host more charged residues without disrupting the trans-protein electric field (Ahern and Horn, 2004; Tombola et al., 2007; González-Pérez et al., 2010). The voltage-sensing domain is energetically linked to the cytosolic end of S6 in the pore domain, mostly through the S4-S5 linker. Open probability increases 20-fold the for every 6-mV depolarization (Aggarwal and MacKinnon, 1996; Seoh et al., 1996; Islas and Sigworth, 1999; Lu et al., 2002; Long et al., 2005b; Batulan et al., 2010; González-Pérez et al., 2010).

In the Shaker Kv channel, residues located toward the internal end of S6 are important for both permeation and electromechanical coupling (Ding and Horn, 2002; Hackos et al., 2002; Sukhareva et al., 2003; Batulan et al., 2010). Because the electromechanical coupling is tight, mutual interference between permeant cations and channel gating is expected. In fact, we've known for a long time that Rb^+ and K^+ slow channel closure in the squid axon and in oocytes, resembling a "foot in the door" mechanism, suggesting the existence of a cation-selective site near the inner end of the pore (Swenson and Armstrong, 1981; Matteson and Swenson, 1986). Such a site was supported by the observation that K^+ ions applied internally lock in quaternary ammonia or Mg^{2+} (Thompson and Begenisich, 2001; Moscoso et al., 2012). Thus, tampering with pore occupancy to increase conductance also affects voltage sensitivity (Sukhareva et al., 2003; Moscoso et al., 2012).

Is it possible that the reduced unitary conductance of Kv channels is a consequence of the tight functional coupling between the voltage sensor and the pore domain? Faure et al. (2012) proposed an ∼4-Å radial displacement during the opening transition based on luminescence resonance energy transfer (LRET) measurements of the bacterial Kv channel, KvAP. This displacement is about the same as the effective radial difference between closed and open pore structures of KcsA and Kv1.2/2.1, respectively (Moldenhauer et al., 2016). Molecular dynamics simulations of Kv1.2-2.1 under an external elec-

tric field show channel openings as small conformational changes at the activation gate. Ensuing pore hydration drives the channel toward its conductive state (Jensen et al., 2012). This process, coined "hydrophobic gating," has been reported for several other ion channels. Small, not physically occluded, pores reside in a de-wetted state because water molecules refuse to interact with their hydrophobic linings (Beckstein et al., 2003; Anishkin and Sukharev, 2004; Jensen et al., 2010, 2012; Zhu and Hummer, 2012a; Neale et al., 2015). The critical radius for pore hydration is ∼4–5 Å, very close to the radius of the internal entrance in the Kv1.2/2.1 structure (Beckstein et al., 2003; Webster et al., 2004; Long et al., 2005b; Wang et al., 2008; Díaz-Franulic et al., 2015). Thus, according to these considerations, pore opening in Kv channels might be barely wide enough to allow permeation.

The closed–open transitions seem to be ruled by economical conformational changes in other ion channels too. In fact, several ion channels (K^+-CNG and TRP) switch between open and closed states with physically small conformational changes in the inner cavity and/or at the selectivity filter (Flynn and Zagotta, 2001; Bruening-Wright et al., 2002; Proks et al., 2003; Salazar et al., 2009; Rapedius et al., 2012; Cao et al., 2013; Garg et al., 2013; Liao et al., 2013; Posson et al., 2013).

Although small movements during channel gating are not mandatory by any biophysical principle, they may possibly result from an evolutionary selective pressure to reduce the energy required to control the pore open probability. Assuming 25–33 cal/mol per $Å^2$ of hydrocarbon exposed to water (Reynolds et al., 1974), a cylindrical greasy cavity of 15-Å depth and 5-Å radius requires 11–15 kcal/mol to open. This figure may be considered a lower limit for the work the electromechanic gear has to perform to open the pore of a Kv channel because it prefers to be closed (Yifrach and MacKinnon, 2002; Jensen et al., 2010, 2012).

On the opposite sidewalk, a large-conductance channel such as BK, endowed with a wider pore, would require larger, energetically expensive gate movements (Beckstein and Sansom, 2004). To open the gate of a BK-like channel, a 7-Å radius pore would require 16–21 kcal/mol, that is 5–6 kcal/mol more than those required to open a Kv channel (Reynolds et al., 1974). If, as recent crystal structures suggest, the Slo2.2 BK channel primary gate is located at the internal bundle crossing, as in Kv channels (Hite et al., 2015), the extra energy required to open BK's pore can be translated into a shift along the voltage axis. The voltage shift, ΔV, is $\Delta V = \Delta\Delta G/zF$, where $\Delta\Delta G$ is the difference between the energies required to open both pores, z is the effective valence of the voltage dependence, and F the Faraday constant. Interestingly, if we take BK's voltage dependency as z = 1.5–2.0, the additional energy required to gate the wider pore would correspond to a positive 100–170-mV shift in the conductance-voltage relationship with respect to Kv channels. Aware that this calculation oversimplifies gating energetics, and assuming similar voltage-responsive gears, it is remarkable that such a voltage shift agrees well with the actual difference in half-activation voltage between BK and Kv channels (Díaz et al., 1998; Horrigan et al., 1999). In addition, other larger-conductance ion channels such as TRPV1 also exhibit similarly shifted conductance-voltage relationships (Matta and Ahern, 2007). Several larger-conductance and multimodal ion channels have evolved additional, physiologically relevant gates, distinct from those at the cytoplasmic end of the pore, which gate ion access with 1–2-Å movements (Flynn and Zagotta, 2001; Bruening-Wright et al., 2002; Proks et al., 2003; Salazar et al., 2009; Rapedius et al., 2012; Garg et al., 2013).

This rationale of small movement gates is per se speculative and simplistic because there aren't obvious biophysical or physiological constraints to limit pore gating to small conformational adjustments. Worse, x-ray structures have to be taken with certain skepticism because they are obtained under nonphysiological conditions. Nevertheless, we should bear in mind that, on the one hand, energy economy is not uncommon in the operation of K^+ channels (for example, in cation coordination in the selectivity filter), and, on the other hand, smaller energy requirements to open the pore would permit a sensitive tuning of the channel open probability.

The physiological role of unitary conductance is mostly unknown

The large functional diversity and regulatory mechanisms of K^+ channels surely underlie physiological fine-tuning within each cell type. These channels are present in almost every tissue, and most cells express different K^+ channels. Possibly, because of this functional redundancy, K^+ channel pathologies are rarely fatal, although they often seriously challenge an individual's happiness. Finding the physiological significance for the spectrum of unitary conductances in K^+ channels is also challenging because there is not a clear connection with cell type. In this regard, congenital channelopathy analysis could inform us about the physiological relevance of unitary conductance if we focus on missense mutations occurring at the internal end of S6, the functional hotspot for conductance and electromechanical coupling (Ding and Horn, 2002; Lu et al., 2002; Sukhareva et al., 2003; Long et al., 2005b; Posson et al., 2013). A myriad of mutations in S6, with pathological consequences, may potentially be affecting unitary conductance (Table 3), but in most cases, research has focused largely on the macroscopic phenotype, such as current density and kinetics, failing to explore microscopic electrophysiological behavior. For example, episodic ataxia type 1 (EA1; characterized by spells of incoordination and imbalance) is caused by mutations in the *KCNA1*

Table 3. **S6 channelopathies of voltage-dependent K^+ channels**

Channel	Gene	Unitary cond.	Tissue expression	S6 limits	Mutation	Disease		Reference
		pS						
Kv1.1	*KCNA1*	8.7–20	Central nervous system, kidney, and heart	387–415	V404I, V408A	Episodic ataxia	EA1	Browne et al., 1994; Scheffer et al., 1998
Kv1.2	*KCNA2*	14–18	Neocortex, hippocampus, main olfactory bulb, and cerebellum	389–417	P405L	Early infantile epileptic encephalopathy, 32	EIEE32	Syrbe et al., 2015
Kv2.1	*KCNB1*	14	Hippocampal neurons and cortical neurons	392–420	G401R	Early infantile epileptic encephalopathy, 26	EIEE26	Saitsu et al., 2015
Kv3.3	*KCNC3*	32–38	Cerebellum, basal ganglia, and spinal cord	518–539	V535M	Spinocerebellar ataxia 13	SCA13	Duarri et al., 2015
Kv4.3	*KCND3*	4	Substantia nigra pars compact, retrosplenial cortex, superior colliculus, the raphe nuclei and amygdala, olfactory bulb, and dentate gyrus	382–402	S390N; V392I	Spinocerebellar ataxia 19; Brugada syndrome	SCA19; BRGDA9	Duarri et al., 2012; Giudicessi et al., 2012
Kv7.1	*KCNQ1*	0.7–4	Heart, uterus, stomach, small and large intestine, kidney and pancreas; smooth muscle	328–348	F339Y, A341E/G/V, L342F, P343L/R/S, A344E/V, G345E/R	Long QT síndrome type 1	LQT1	Jongbloed et al., 1999; Tester et al., 2005; Kapplinger et al., 2009
Kv7.2	*KCNQ2*	6.5	Hippocampal and cortical neurons	292–312	A306T	Benign familial neonatal seizures	BFNS1	Singh et al., 2003
Kv7.4	*KCNQ4*	2.1	Brain, cochlea, heart, and skeletal muscle; neuron derived from embryonic stem cells	297–317	G321S	Deafness autosomal dominant 2A	DFNA2A	Coucke et al., 1999
Kv10.1 EAG	*KCNH1*	8.5	Brain, kidney, lung, and pancreas; in brain: in cortex, hippocampus, caudate, putamen, amígdala, and substantia nigra	478–498	L489F, I494V	Temple-Baraitser syndrome and epilepsy	TMBTS	Simons et al., 2015
Kv11.1 ERG	*KCNH2*	10–13	Brian: reticular thalamic nucleus, cerebral cortex, cerebellum, and hippocampus; heart	639–659	F640L/V, S641F, V644F/L, M645I/L, G648S, F656C, G657R	Long QT syndrome 2	LGT2	Napolitano et al., 2005; Tester et al., 2005; Kapplinger et al., 2009
KCa3.1	*KCNN4*	30–80	Nonexcitable tissues	265–285	V282E/M	Dehydrated hereditary stomatocytosis	DHS2	Glogowska et al., 2015
TASK 3	*KCNK9*	16–32	Cerebellum and external plexiform layer of the olfactory bulb; hippocampus	219–239	G236R	Birk-Barel mental retardation dysmorphism	BIBAS	Barel et al., 2008

Non-exhaustive listing of mutations potentially affecting unitary conductance in voltage-gated K^+ channel. Mutational data as well as topological composition of S6 transmembrane segments were obtained from UniProt (http://www.uniprot.org/uniprot/).

gene (Kv1.1). Likewise, cerebellar ataxia (CA), characterized by coordination imbalance, and epileptic encephalopathy early infantile 32 (EIEE32), characterized by refractory seizures and neurodevelopmental impairment, are both caused by mutation of the *KCNA2* gene (Kv1.2; Imbrici et al., 2006; Xie et al., 2010; Syrbe et al., 2015). Mutations could diminish ionic currents by decreasing protein maturation, trafficking, or activity level, or interaction with accessory subunits, and/or by dominant-negative effects. Nevertheless, we will miss the whole pathological picture as long as we ignore their impact on unitary conductance.

We must not think that the unitary conductance is a fixed character of the channel. There are beautiful examples of how accessory subunits change conductance. For example, the unitary conductances of Kv4.2 and Kv7.1 (*KCNQ1*) increase several fold when they are coexpressed with accessory subunits: dipeptidyl-peptidase–like protein-6 (DPP6) and *KCNE1* (MinK), respectively (Melman et al., 2004; Kaulin et al., 2009). The mechanism behind this DPP6 gain of function is similar to that of the Glu ring in BK (Kaulin et al., 2009), whereas in MinK it seems to involve intimate interaction with the S6 domain of Kv7 (Melman et al., 2004). Are these changes

in unitary conductance relevant or just collateral consequences of the protein–protein interaction controlling gating kinetics and inactivation? By dissociating kinetics from conductance phenotypes, these cases present an opportunity to understand how relevant the changes in the unitary conductance are to physiology.

Concluding remarks

K^+ channels are finely tuned to allow the selective passage of K^+ across the membrane at high rates. The channel selectivity filter is in charge of this task, dropping to near zero the energy for ion transfer from the bulk solution (Morais-Cabral et al., 2001). K^+ ions pass across the selectivity filter so efficiently that, even in the largest conductance channels, the physical dimensions of the internal vestibule limit channel conductance (Geng et al., 2011). Thus, we propose that the main difference between large- and small-conductance channels arises from the size of the entrance to the internal pore; large-conductance channels have wider vestibules than do smaller conductance ones. The effect of vestibule size on unitary conductance is clearly nonsteric because it is not proportional to the sectional area available for permeation. Inside narrow aqueous pores, embedded in low dielectric lipid membranes, ions require larger energies to become stabilized, limiting K^+ current (Parsegian, 1969). These equilibrium energy considerations would reduce the conductance gap from approximately two orders of magnitude to one third of the maximal transport rate, corresponding to ∼1 *k*T in activation energy terms. The rest of the difference remains to be accounted for (Díaz-Franulic et al., 2015). Although Kv channels open just wide enough to let hydrated ions enter the permeation pathway, larger-conductance channels would require larger energies to open because of the hydrophobic nature of their inner walls. Thus, larger-conductance channels may host other activation gates as functional and structural data suggest (Zhou et al., 2011; Hite et al., 2015). Because structural determinants for unitary conductance and for electromechanical coupling colocalize toward the cytosolic end of S6, a mutual interference between pore occupancy and gating is expected. Therefore, S6 mutant Kv channelopathies require unitary conductance studies to fully understand their pathophysiology.

ACKNOWLEDGMENTS

We thank John Ewer (Centro Interdisciplinario de Neurociencia de Valparaíso [CINV]) for critical reading of the manuscript.

This work is supported by Fondo Nacional de Desarrollo Científico y Tecnológico (Fondecyt) grant #1120819 and by Iniciativa Cientifica Milenio grant PO9-022. I. Díaz-Franulic and H. Moldenhauer were funded by Fraunhofer Chile Research and Fondecyt postdoctoral grant #3160321, respectively. The CINV is a Millennium Institute supported by the Millennium Scientific Initiative of the Ministerio de Economía, Fomento y Turismo.

The authors declare no competing financial interests.
Lesley C. Anson served as editor.

Submitted: 19 May 2016
Accepted: 10 August 2016

REFERENCES

Aggarwal, S.K., and R. MacKinnon. 1996. Contribution of the S4 segment to gating charge in the *Shaker* K^+ channel. *Neuron.* 16:1169–1177. http://dx.doi.org/10.1016/S0896-6273(00)80143-9

Ahern, C.A., and R. Horn. 2004. Specificity of charge-carrying residues in the voltage sensor of potassium channels. *J. Gen. Physiol.* 123:205–216. http://dx.doi.org/10.1085/jgp.200308993

Alam, A., and Y. Jiang. 2009. High-resolution structure of the open NaK channel. *Nat. Struct. Mol. Biol.* 16:30–34. http://dx.doi.org/10.1038/nsmb.1531

Alcayaga, C., X. Cecchi, O. Alvarez, and R. Latorre. 1989. Streaming potential measurements in Ca2+-activated K+ channels from skeletal and smooth muscle. Coupling of ion and water fluxes. *Biophys. J.* 55:367–371. http://dx.doi.org/10.1016/S0006-3495(89)82814-0

Allen, T.W., O.S. Andersen, and B. Roux. 2004. On the importance of atomic fluctuations, protein flexibility, and solvent in ion permeation. *J. Gen. Physiol.* 124:679–690. http://dx.doi.org/10.1085/jgp.200409111

Andersen, O.S. 1983. Ion movement through gramicidin A channels. Studies on the diffusion-controlled association step. *Biophys. J.* 41:147–165. http://dx.doi.org/10.1016/S0006-3495(83)84416-6

Anishkin, A., and S. Sukharev. 2004. Water dynamics and dewetting transitions in the small mechanosensitive channel MscS. *Biophys. J.* 86:2883–2895. http://dx.doi.org/10.1016/S0006-3495(04)74340-4

Åqvist, J., and V. Luzhkov. 2000. Ion permeation mechanism of the potassium channel. *Nature.* 404:881–884. http://dx.doi.org/10.1038/35009114

Armstrong, C.M. 1971. Interaction of tetraethylammonium ion derivatives with the potassium channels of giant axons. *J. Gen. Physiol.* 58:413–437. http://dx.doi.org/10.1085/jgp.58.4.413

Armstrong, C.M. 2015. Packaging life: the origin of ion-selective channels. *Biophys. J.* 109:173–177. http://dx.doi.org/10.1016/j.bpj.2015.06.012

Bankura, A., V. Carnevale, and M.L. Klein. 2013. Hydration structure of salt solutions from ab initio molecular dynamics. *J. Chem. Phys.* 138:014501. http://dx.doi.org/10.1063/1.4772761

Barel, O., S.A. Shalev, R. Ofir, A. Cohen, J. Zlotogora, Z. Shorer, G. Mazor, G. Finer, S. Khateeb, N. Zilberberg, and O.S. Birk. 2008. Maternally inherited Birk Barel mental retardation dysmorphism syndrome caused by a mutation in the genomically imprinted potassium channel KCNK9. *Am. J. Hum. Genet.* 83:193–199. http://dx.doi.org/10.1016/j.ajhg.2008.07.010

Batulan, Z., G.A. Haddad, and R. Blunck. 2010. An intersubunit interaction between S4-S5 linker and S6 is responsible for the slow off-gating component in Shaker K^+ channels. *J. Biol. Chem.* 285:14005–14019. http://dx.doi.org/10.1074/jbc.M109.097717

Beckstein, O., and M.S. Sansom. 2004. The influence of geometry, surface character, and flexibility on the permeation of ions and water through biological pores. *Phys. Biol.* 1:42–52. http://dx.doi.org/10.1088/1478-3967/1/1/005

Beckstein, O., P.C. Biggin, P. Bond, J.N. Bright, C. Domene, A. Grottesi, J. Holyoake, and M.S. Sansom. 2003. Ion channel gating: insights via molecular simulations. *FEBS Lett.* 555:85–90. http://dx.doi.org/10.1016/S0014-5793(03)01151-7

Bernèche, S., and B. Roux. 2000. Molecular dynamics of the KcsA K^+ channel in a bilayer membrane. *Biophys. J.* 78:2900–2917. http://dx.doi.org/10.1016/S0006-3495(00)76831-7

Bernèche, S., and B. Roux. 2003. A microscopic view of ion conduction through the K+ channel. *Proc. Natl. Acad. Sci. USA.* 100:8644–8648. http://dx.doi.org/10.1073/pnas.1431750100

Bezanilla, F., and C.M. Armstrong. 1972. Negative conductance caused by entry of sodium and cesium ions into the potassium channels of squid axons. *J. Gen. Physiol.* 60:588–608. http://dx.doi.org/10.1085/jgp.60.5.588

Brelidze, T.I., and K.L. Magleby. 2005. Probing the geometry of the inner vestibule of BK channels with sugars. *J. Gen. Physiol.* 126:105–121. http://dx.doi.org/10.1085/jgp.200509286

Brelidze, T.I., X. Niu, and K.L. Magleby. 2003. A ring of eight conserved negatively charged amino acids doubles the conductance of BK channels and prevents inward rectification. *Proc. Natl. Acad. Sci. USA.* 100:9017–9022. http://dx.doi.org/10.1073/pnas.1532257100

Browne, D.L., S.T. Gancher, J.G. Nutt, E.R. Brunt, E.A. Smith, P. Kramer, and M. Litt. 1994. Episodic ataxia/myokymia syndrome is associated with point mutations in the human potassium channel gene, KCNA1. *Nat. Genet.* 8:136–140. http://dx.doi.org/10.1038/ng1094-136

Bruening-Wright, A., M.A. Schumacher, J.P. Adelman, and J. Maylie. 2002. Localization of the activation gate for small conductance Ca^{2+}-activated K^+ channels. *J. Neurosci.* 22:6499–6506.

Budelli, G., Y. Geng, A. Butler, K.L. Magleby, and L. Salkoff. 2013. Properties of Slo1 K^+ channels with and without the gating ring. *Proc. Natl. Acad. Sci. USA.* 110:16657–16662. http://dx.doi.org/10.1073/pnas.1313433110

Cao, E., M. Liao, Y. Cheng, and D. Julius. 2013. TRPV1 structures in distinct conformations reveal activation mechanisms. *Nature.* 504:113–118. http://dx.doi.org/10.1038/nature12823

Carrasquel-Ursulaez, W., G.F. Contreras, R.V. Sepúlveda, D. Aguayo, F. González-Nilo, C. González, and R. Latorre. 2015. Hydrophobic interaction between contiguous residues in the S6 transmembrane segment acts as a stimuli integration node in the BK channel. *J. Gen. Physiol.* 145:61–74. http://dx.doi.org/10.1085/jgp.201411194

Carvacho, I., W. Gonzalez, Y.P. Torres, S. Brauchi, O. Alvarez, F.D. Gonzalez-Nilo, and R. Latorre. 2008. Intrinsic electrostatic potential in the BK channel pore: role in determining single channel conductance and block. *J. Gen. Physiol.* 131:147–161. http://dx.doi.org/10.1085/jgp.200709862

Chen, H., F.C. Chatelain, and F. Lesage. 2014. Altered and dynamic ion selectivity of K^+ channels in cell development and excitability. *Trends Pharmacol. Sci.* 35:461–469. http://dx.doi.org/10.1016/j.tips.2014.06.002

Cheng, W.W., J.G. McCoy, A.N. Thompson, C.G. Nichols, and C.M. Nimigean. 2011. Mechanism for selectivity-inactivation coupling in KcsA potassium channels. *Proc. Natl. Acad. Sci. USA.* 108:5272–5277. http://dx.doi.org/10.1073/pnas.1014186108

Chung, S.H., T.W. Allen, and S. Kuyucak. 2002. Conducting-state properties of the KcsA potassium channel from molecular and Brownian dynamics simulations. *Biophys. J.* 82:628–645. http://dx.doi.org/10.1016/S0006-3495(02)75427-1

Contreras, J.E., J. Chen, A.Y. Lau, V. Jogini, B. Roux, and M. Holmgren. 2010. Voltage profile along the permeation pathway of an open channel. *Biophys. J.* 99:2863–2869. http://dx.doi.org/10.1016/j.bpj.2010.08.053

Coucke, P.J., P. Van Hauwe, P.M. Kelley, H. Kunst, I. Schatteman, D. Van Velzen, J. Meyers, R.J. Ensink, M. Verstreken, F. Declau, et al. 1999. Mutations in the KCNQ4 gene are responsible for autosomal dominant deafness in four DFNA2 families. *Hum. Mol. Genet.* 8:1321–1328. http://dx.doi.org/10.1093/hmg/8.7.1321

Cuello, L.G., V. Jogini, D.M. Cortes, and E. Perozo. 2010. Structural mechanism of C-type inactivation in K^+ channels. *Nature.* 466:203–208. http://dx.doi.org/10.1038/nature09153

del Camino, D., M. Kanevsky, and G. Yellen. 2005. Status of the intracellular gate in the activated-not-open state of Shaker K^+ channels. *J. Gen. Physiol.* 126:419–428. http://dx.doi.org/10.1085/jgp.200509385

Derebe, M.G., D.B. Sauer, W. Zeng, A. Alam, N. Shi, and Y. Jiang. 2011. Tuning the ion selectivity of tetrameric cation channels by changing the number of ion binding sites. *Proc. Natl. Acad. Sci. USA.* 108:598–602. http://dx.doi.org/10.1073/pnas.1013636108

Díaz, L., P. Meera, J. Amigo, E. Stefani, O. Alvarez, L. Toro, and R. Latorre. 1998. Role of the S4 segment in a voltage-dependent calcium-sensitive potassium (hSlo) channel. *J. Biol. Chem.* 273:32430–32436. http://dx.doi.org/10.1074/jbc.273.49.32430

Díaz-Franulic, I., R.V. Sepúlveda, N. Navarro-Quezada, F. González-Nilo, and D. Naranjo. 2015. Pore dimensions and the role of occupancy in unitary conductance of Shaker K channels. *J. Gen. Physiol.* 146:133–146. http://dx.doi.org/10.1085/jgp.201411353

Ding, S., and R. Horn. 2002. Tail end of the S6 segment: role in permeation in Shaker potassium channels. *J. Gen. Physiol.* 120:87–97. http://dx.doi.org/10.1085/jgp.20028611

Doyle, D.A., J. Morais Cabral, R.A. Pfuetzner, A. Kuo, J.M. Gulbis, S.L. Cohen, B.T. Chait, and R. MacKinnon. 1998. The structure of the potassium channel: molecular basis of K^+ conduction and selectivity. *Science.* 280:69–77. http://dx.doi.org/10.1126/science.280.5360.69

Duarri, A., J. Jezierska, M. Fokkens, M. Meijer, H.J. Schelhaas, W.F. den Dunnen, F. van Dijk, C. Verschuuren-Bemelmans, G. Hageman, P. van de Vlies, et al. 2012. Mutations in potassium channel kcnd3 cause spinocerebellar ataxia type 19. *Ann. Neurol.* 72:870–880. http://dx.doi.org/10.1002/ana.23700

Duarri, A., E.A. Nibbeling, M.R. Fokkens, M. Meijer, M. Boerrigter, C.C. Verschuuren-Bemelmans, B.P. Kremer, B.P. van de Warrenburg, D. Dooijes, E. Boddeke, et al. 2015. Functional analysis helps to define KCNC3 mutational spectrum in Dutch ataxia cases. *PLoS One.* 10:e0116599. http://dx.doi.org/10.1371/journal.pone.0116599

Eisenberg, B. 2013. Interacting ions in biophysics: real is not ideal. *Biophys. J.* 104:1849–1866. http://dx.doi.org/10.1016/j.bpj.2013.03.049

Eisenman, G. 1962. Cation selective glass electrodes and their mode of operation. *Biophys. J.* 2:259–323. http://dx.doi.org/10.1016/S0006-3495(62)86959-8

Eisenman, G., R. Latorre, and C. Miller. 1986. Multi-ion conduction and selectivity in the high-conductance Ca++-activated K+ channel from skeletal muscle. *Biophys. J.* 50:1025–1034. http://dx.doi.org/10.1016/S0006-3495(86)83546-9

Enderby, J.E. 1995. Ion solvation via neutron scattering. *Chem. Soc. Rev.* 24:159–168. http://dx.doi.org/10.1039/cs9952400159

Faure, É., G. Starek, H. McGuire, S. Bernèche, and R. Blunck. 2012. A limited 4 Å radial displacement of the S4-S5 linker is sufficient for internal gate closing in Kv channels. *J. Biol. Chem.* 287:40091–40098. http://dx.doi.org/10.1074/jbc.M112.415497

Ferry, J.D. 1936. Statistical evaluation of sieve constants in ultrafiltration. *J. Gen. Physiol.* 20:95–104. http://dx.doi.org/10.1085/jgp.20.1.95

Flynn, G.E., and W.N. Zagotta. 2001. Conformational changes in S6 coupled to the opening of cyclic nucleotide-gated channels. *Neuron.* 30:689–698. http://dx.doi.org/10.1016/S0896-6273(01)00324-5

Garate, J.A., T. Perez-Acle, and C. Oostenbrink. 2014. On the thermodynamics of carbon nanotube single-file water loading: free energy, energy and entropy calculations. *Phys. Chem. Chem. Phys.* 16:5119–5128. http://dx.doi.org/10.1039/c3cp54554g

Garg, P., A. Gardner, V. Garg, and M.C. Sanguinetti. 2013. Structural basis of ion permeation gating in Slo2.1 K^+ channels. *J. Gen. Physiol.* 142:523–542. http://dx.doi.org/10.1085/jgp.201311064

Geng, Y., X. Niu, and K.L. Magleby. 2011. Low resistance, large dimension entrance to the inner cavity of BK channels determined by changing side-chain volume. *J. Gen. Physiol.* 137:533–548. http://dx.doi.org/10.1085/jgp.201110616

Giudicessi, J.R., D. Ye, C.J. Kritzberger, V.V. Nesterenko, D.J. Tester, C. Antzelevitch, and M.J. Ackerman. 2012. Novel mutations in the *KCND3*-encoded Kv4.3 K^+ channel associated with autopsy-negative sudden unexplained death. *Hum. Mutat.* 33:989–997. http://dx.doi.org/10.1002/humu.22058

Glezakou, V.-A., Y. Chen, J.L. Fulton, G.K. Schenter, and L.X. Dang. 2006. Electronic structure, statistical mechanical simulations, and EXAFS spectroscopy of aqueous potassium. *Theor. Chem. Acc.* 115:86–99. http://dx.doi.org/10.1007/s00214-005-0054-4

Glogowska, E., K. Lezon-Geyda, Y. Maksimova, V.P. Schulz, and P.G. Gallagher. 2015. Mutations in the Gardos channel (KCNN4) are associated with hereditary xerocytosis. *Blood.* 126:1281–1284. http://dx.doi.org/10.1182/blood-2015-07-657957

González-Pérez, V., K. Stack, K. Boric, and D. Naranjo. 2010. Reduced voltage sensitivity in a K^+-channel voltage sensor by electric field remodeling. *Proc. Natl. Acad. Sci. USA.* 107:5178–5183. http://dx.doi.org/10.1073/pnas.1000963107

Grossfield, A. 2005. Dependence of ion hydration on the sign of the ion's charge. *J. Chem. Phys.* 122:024506. http://dx.doi.org/10.1063/1.1829036

Gutman, G.A., K.G. Chandy, S. Grissmer, M. Lazdunski, D. McKinnon, L.A. Pardo, G.A. Robertson, B. Rudy, M.C. Sanguinetti, W. Stühmer, and X. Wang. 2005. International Union of Pharmacology. LIII. Nomenclature and molecular relationships of voltage-gated potassium channels. *Pharmacol. Rev.* 57:473–508. http://dx.doi.org/10.1124/pr.57.4.10

Hackos, D.H., T.H. Chang, and K.J. Swartz. 2002. Scanning the intracellular S6 activation gate in the shaker K^+ channel. *J. Gen. Physiol.* 119:521–531. http://dx.doi.org/10.1085/jgp.20028569

Heginbotham, L., and R. MacKinnon. 1993. Conduction properties of the cloned Shaker K+ channel. *Biophys. J.* 65:2089–2096. http://dx.doi.org/10.1016/S0006-3495(93)81244-X

Heginbotham, L., Z. Lu, T. Abramson, and R. MacKinnon. 1994. Mutations in the K+ channel signature sequence. *Biophys. J.* 66:1061–1067. http://dx.doi.org/10.1016/S0006-3495(94)80887-2

Hille, B. 1973. Potassium channels in myelinated nerve. Selective permeability to small cations. *J. Gen. Physiol.* 61:669–686. http://dx.doi.org/10.1085/jgp.61.6.669

Hille, B. 2001. Ion channels of excitable membranes. Third edition. Sinauer, Sunderland, MA. 814 pp.

Hite, R.K., P. Yuan, Z. Li, Y. Hsuing, T. Walz, and R. MacKinnon. 2015. Cryo-electron microscopy structure of the Slo2.2 Na^+-activated K^+ channel. *Nature.* 527:198–203. http://dx.doi.org/10.1038/nature14958

Hodgkin, A.L., and A.F. Huxley. 1952. A quantitative description of membrane current and its application to conduction and excitation in nerve. *J. Physiol.* 117:500–544. http://dx.doi.org/10.1113/jphysiol.1952.sp004764

Hodgkin, A.L., and R.D. Keynes. 1955. The potassium permeability of a giant nerve fibre. *J. Physiol.* 128:61–88. http://dx.doi.org/10.1113/jphysiol.1955.sp005291

Horrigan, F.T., J. Cui, and R.W. Aldrich. 1999. Allosteric voltage gating of potassium channels I. Mslo ionic currents in the absence of Ca^{2+}. *J. Gen. Physiol.* 114:277–304. http://dx.doi.org/10.1085/jgp.114.2.277

Humphrey, W., A. Dalke, and K. Schulten. 1996. VMD: Visual molecular dynamics. *J. Mol. Graph.* 14:33–38.

Imbrici, P., M.C. D'Adamo, D.M. Kullmann, and M. Pessia. 2006. Episodic ataxia type 1 mutations in the *KCNA1* gene impair the fast inactivation properties of the human potassium channels Kv1.4-1.1/Kvβ1.1 and Kv1.4-1.1/Kvβ1.2. *Eur. J. Neurosci.* 24:3073–3083. http://dx.doi.org/10.1111/j.1460-9568.2006.05186.x

Islas, L.D., and F.J. Sigworth. 1999. Voltage sensitivity and gating charge in Shaker and Shab family potassium channels. *J. Gen. Physiol.* 114:723–742. http://dx.doi.org/10.1085/jgp.114.5.723

Jensen, M.O., D.W. Borhani, K. Lindorff-Larsen, P. Maragakis, V. Jogini, M.P. Eastwood, R.O. Dror, and D.E. Shaw. 2010. Principles of conduction and hydrophobic gating in K^+ channels. *Proc. Natl. Acad. Sci. USA.* 107:5833–5838. http://dx.doi.org/10.1073/pnas.0911691107

Jensen, M.O., V. Jogini, D.W. Borhani, A.E. Leffler, R.O. Dror, and D.E. Shaw. 2012. Mechanism of voltage gating in potassium channels. *Science.* 336:229–233. http://dx.doi.org/10.1126/science.1216533

Jensen, M.O., V. Jogini, M.P. Eastwood, and D.E. Shaw. 2013. Atomic-level simulation of current-voltage relationships in single-file ion channels. *J. Gen. Physiol.* 141:619–632. http://dx.doi.org/10.1085/jgp.201210820

Jiang, Y., A. Lee, J. Chen, M. Cadene, B.T. Chait, and R. MacKinnon. 2002. Crystal structure and mechanism of a calcium-gated potassium channel. *Nature.* 417:515–522. http://dx.doi.org/10.1038/417515a

Jogini, V., and B. Roux. 2005. Electrostatics of the intracellular vestibule of K^+ channels. *J. Mol. Biol.* 354:272–288. http://dx.doi.org/10.1016/j.jmb.2005.09.031

Jongbloed, R.J., A.A. Wilde, J.L. Geelen, P. Doevendans, C. Schaap, I. Van Langen, J.P. van Tintelen, J.M. Cobben, G.C. Beaufort-Krol, J.P. Geraedts, and H.J. Smeets. 1999. Novel KCNQ1 and HERG missense mutations in Dutch long-QT families. *Hum. Mutat.* 13:301–310. http://dx.doi.org/10.1002/(SICI)1098-1004(1999)13:4<301::AID-HUMU7>3.0.CO;2-V

Kapplinger, J.D., D.J. Tester, B.A. Salisbury, J.L. Carr, C. Harris-Kerr, G.D. Pollevick, A.A. Wilde, and M.J. Ackerman. 2009. Spectrum and prevalence of mutations from the first 2,500 consecutive unrelated patients referred for the FAMILION long QT syndrome genetic test. *Heart Rhythm.* 6:1297–1303. http://dx.doi.org/10.1016/j.hrthm.2009.05.021

Kaulin, Y.A., J.A. De Santiago-Castillo, C.A. Rocha, M.S. Nadal, B. Rudy, and M. Covarrubias. 2009. The dipeptidyl-peptidase-like protein DPP6 determines the unitary conductance of neuronal Kv4.2 channels. *J. Neurosci.* 29:3242–3251. http://dx.doi.org/10.1523/JNEUROSCI.4767-08.2009

Kobertz, W.R., and C. Miller. 1999. K+ channels lacking the 'tetramerization' domain: implications for pore structure. *Nat. Struct. Biol.* 6:1122–1125. http://dx.doi.org/10.1038/70061

Krishnamoorthy, G., J. Shi, D. Sept, and J. Cui. 2005. The NH_2 terminus of RCK1 domain regulates Ca^{2+}-dependent BK_{Ca} channel gating. *J. Gen. Physiol.* 126:227–241. http://dx.doi.org/10.1085/jgp.200509321

Latorre, R., and C. Miller. 1983. Conduction and selectivity in potassium channels. *J. Membr. Biol.* 71:11–30. http://dx.doi.org/10.1007/BF01870671

Läuger, P. 1976. Diffusion-limited ion flow through pores. *Biochim. Biophys. Acta.* 455:493–509. http://dx.doi.org/10.1016/0005-2736(76)90320-5

Li, W., and R.W. Aldrich. 2004. Unique inner pore properties of BK channels revealed by quaternary ammonium block. *J. Gen. Physiol.* 124:43–57. http://dx.doi.org/10.1085/jgp.200409067

Liao, M., E. Cao, D. Julius, and Y. Cheng. 2013. Structure of the TRPV1 ion channel determined by electron cryo-microscopy. *Nature*. 504:107–112. http://dx.doi.org/10.1038/nature12822

Liu, S., and S.W. Lockless. 2013. Equilibrium selectivity alone does not create K^+-selective ion conduction in K^+ channels. *Nat. Commun*. 4:2746.

Liu, S., X. Bian, and S.W. Lockless. 2012. Preferential binding of K^+ ions in the selectivity filter at equilibrium explains high selectivity of K^+ channels. *J. Gen. Physiol.* 140:671–679. http://dx.doi.org/10.1085/jgp.201210855

Lockless, S.W. 2015. Determinants of cation transport selectivity: Equilibrium binding and transport kinetics. *J. Gen. Physiol.* 146:3–13. http://dx.doi.org/10.1085/jgp.201511371

Long, S.B., E.B. Campbell, and R. Mackinnon. 2005a. Crystal structure of a mammalian voltage-dependent *Shaker* family K^+ channel. *Science*. 309:897–903. http://dx.doi.org/10.1126/science.1116269

Long, S.B., E.B. Campbell, and R. Mackinnon. 2005b. Voltage sensor of Kv1.2: structural basis of electromechanical coupling. *Science*. 309:903–908. http://dx.doi.org/10.1126/science.1116270

Long, S.B., X. Tao, E.B. Campbell, and R. MacKinnon. 2007. Atomic structure of a voltage-dependent K^+ channel in a lipid membrane-like environment. *Nature*. 450:376–382. http://dx.doi.org/10.1038/nature06265

Lu, Z. 2004. Mechanism of rectification in inward-rectifier K^+ channels. *Annu. Rev. Physiol.* 66:103–129. http://dx.doi.org/10.1146/annurev.physiol.66.032102.150822

Lu, Z., A.M. Klem, and Y. Ramu. 2002. Coupling between voltage sensors and activation gate in voltage-gated K^+ channels. *J. Gen. Physiol.* 120:663–676. http://dx.doi.org/10.1085/jgp.20028696

Mancinelli, R., A. Botti, F. Bruni, M.A. Ricci, and A.K. Soper. 2007. Hydration of sodium, potassium, and chloride ions in solution and the concept of structure maker/breaker. *J. Phys. Chem. B*. 111:13570–13577. http://dx.doi.org/10.1021/jp075913v

Matta, J.A., and G.P. Ahern. 2007. Voltage is a partial activator of rat thermosensitive TRP channels. *J. Physiol.* 585:469–482. http://dx.doi.org/10.1113/jphysiol.2007.144287

Matteson, D.R., and R.P. Swenson Jr. 1986. External monovalent cations that impede the closing of K channels. *J. Gen. Physiol.* 87:795–816. http://dx.doi.org/10.1085/jgp.87.5.795

Melman, Y.F., S.Y. Um, A. Krumerman, A. Kagan, and T.V. McDonald. 2004. KCNE1 binds to the KCNQ1 pore to regulate potassium channel activity. *Neuron*. 42:927–937. http://dx.doi.org/10.1016/j.neuron.2004.06.001

Miller, C. 1982. Bis-quaternary ammonium blockers as structural probes of the sarcoplasmic reticulum K+ channel. *J. Gen. Physiol.* 79:869–891. http://dx.doi.org/10.1085/jgp.79.5.869

Miller, C. 2001. See potassium run. *Nature*. 414:23–24. http://dx.doi.org/10.1038/35102126

Moldenhauer, H., I. Díaz-Franulic, F. González-Nilo, and D. Naranjo. 2016. Effective pore size and radius of capture for K^+ ions in K-channels. *Sci. Rep.* 6:19893. http://dx.doi.org/10.1038/srep19893

Morais-Cabral, J.H., Y. Zhou, and R. MacKinnon. 2001. Energetic optimization of ion conduction rate by the K^+ selectivity filter. *Nature*. 414:37–42. http://dx.doi.org/10.1038/35102000

Moscoso, C., A. Vergara-Jaque, V. Márquez-Miranda, R.V. Sepúlveda, I. Valencia, I. Díaz-Franulic, F. González-Nilo, and D. Naranjo. 2012. K^+ conduction and Mg^{2+} blockade in a shaker Kv-channel single point mutant with an unusually high conductance. *Biophys. J.* 103:1198–1207. http://dx.doi.org/10.1016/j.bpj.2012.08.015

Mullins, L.J. 1959. An analysis of conductance changes in squid axon. *J. Gen. Physiol.* 42:1013–1035. http://dx.doi.org/10.1085/jgp.42.5.1013

Napolitano, C., S.G. Priori, P.J. Schwartz, R. Bloise, E. Ronchetti, J. Nastoli, G. Bottelli, M. Cerrone, and S. Leonardi. 2005. Genetic testing in the long QT syndrome: development and validation of an efficient approach to genotyping in clinical practice. *JAMA*. 294:2975–2980. http://dx.doi.org/10.1001/jama.294.23.2975

Neale, C., N. Chakrabarti, P. Pomorski, E.F. Pai, and R. Pomès. 2015. Hydrophobic gating of ion permeation in magnesium channel CorA. *PLOS Comput. Biol.* 11:e1004303. http://dx.doi.org/10.1371/journal.pcbi.1004303

Neyton, J., and C. Miller. 1988. Discrete Ba^{2+} block as a probe of ion occupancy and pore structure in the high-conductance Ca^{2+}-activated K^+ channel. *J. Gen. Physiol.* 92:569–586. http://dx.doi.org/10.1085/jgp.92.5.569

Nimigean, C.M., and T.W. Allen. 2011. Origins of ion selectivity in potassium channels from the perspective of channel block. *J. Gen. Physiol.* 137:405–413. http://dx.doi.org/10.1085/jgp.201010551

Nimigean, C.M., J.S. Chappie, and C. Miller. 2003. Electrostatic tuning of ion conductance in potassium channels. *Biochemistry*. 42:9263–9268. http://dx.doi.org/10.1021/bi0348720

Nishida, M., and R. MacKinnon. 2002. Structural basis of inward rectification: cytoplasmic pore of the G protein-gated inward rectifier GIRK1 at 1.8 Å resolution. *Cell*. 111:957–965. http://dx.doi.org/10.1016/S0092-8674(02)01227-8

Noskov, S.Y., and B. Roux. 2006. Ion selectivity in potassium channels. *Biophys. Chem.* 124:279–291. http://dx.doi.org/10.1016/j.bpc.2006.05.033

Noskov, S.Y., S. Bernèche, and B. Roux. 2004. Control of ion selectivity in potassium channels by electrostatic and dynamic properties of carbonyl ligands. *Nature*. 431:830–834. http://dx.doi.org/10.1038/nature02943

Parsegian, A. 1969. Energy of an ion crossing a low dielectric membrane: solutions to four relevant electrostatic problems. *Nature*. 221:844–846. http://dx.doi.org/10.1038/221844a0

Peter, C., and G. Hummer. 2005. Ion transport through membrane-spanning nanopores studied by molecular dynamics simulations and continuum electrostatics calculations. *Biophys. J.* 89:2222–2234. http://dx.doi.org/10.1529/biophysj.105.065946

Piasta, K.N., D.L. Theobald, and C. Miller. 2011. Potassium-selective block of barium permeation through single KcsA channels. *J. Gen. Physiol.* 138:421–436. http://dx.doi.org/10.1085/jgp.201110684

Posson, D.J., J.G. McCoy, and C.M. Nimigean. 2013. The voltage-dependent gate in MthK potassium channels is located at the selectivity filter. *Nat. Struct. Mol. Biol.* 20:159–166. http://dx.doi.org/10.1038/nsmb.2473

Proks, P., J.F. Antcliff, and F.M. Ashcroft. 2003. The ligand-sensitive gate of a potassium channel lies close to the selectivity filter. *EMBO Rep.* 4:70–75. http://dx.doi.org/10.1038/sj.embor.embor708

Rapedius, M., M.R. Schmidt, C. Sharma, P.J. Stansfeld, M.S. Sansom, T. Baukrowitz, and S.J. Tucker. 2012. State-independent intracellular access of quaternary ammonium blockers to the pore of TREK-1. *Channels (Austin)*. 6:473–478. http://dx.doi.org/10.4161/chan.22153

Reynolds, J.A., D.B. Gilbert, and C. Tanford. 1974. Empirical correlation between hydrophobic free energy and aqueous cavity surface area. *Proc. Natl. Acad. Sci. USA*. 71:2925–2927. http://dx.doi.org/10.1073/pnas.71.8.2925

Robinson, R.A., and R.H. Stokes. 2002. Electrolyte solutions. Second revised edition. Dover Publications, Mineola, NY. 590 pp.

Ruta, V., Y. Jiang, A. Lee, J. Chen, and R. MacKinnon. 2003. Functional analysis of an archaebacterial voltage-dependent K^+ channel. *Nature*. 422:180–185. http://dx.doi.org/10.1038/nature01473

Sack, J.T., and D.C. Tilley. 2015. What keeps Kv channels small? The molecular physiology of modesty. *J. Gen. Physiol.* 146:123–127. http://dx.doi.org/10.1085/jgp.201511469

Saitsu, H., T. Akita, J. Tohyama, H. Goldberg-Stern, Y. Kobayashi, R. Cohen, M. Kato, C. Ohba, S. Miyatake, Y. Tsurusaki, et al. 2015. De novo KCNB1 mutations in infantile epilepsy inhibit repetitive neuronal firing. *Sci. Rep.* 5:15199. http://dx.doi.org/10.1038/srep15199

Salazar, H., A. Jara-Oseguera, E. Hernández-García, I. Llorente, I.I. Arias-Olguín, M. Soriano-García, L.D. Islas, and T. Rosenbaum. 2009. Structural determinants of gating in the TRPV1 channel. *Nat. Struct. Mol. Biol.* 16:704–710. http://dx.doi.org/10.1038/nsmb.1633

Sauer, D.B., W. Zeng, J. Canty, Y. Lam, and Y. Jiang. 2013. Sodium and potassium competition in potassium-selective and non-selective channels. *Nat. Commun.* 4:2721. http://dx.doi.org/10.1038/ncomms3721

Scheffer, H., E.R. Brunt, G.J. Mol, P. van der Vlies, R.P. Stulp, E. Verlind, G. Mantel, Y.N. Averyanov, R.M. Hofstra, and C.H. Buys. 1998. Three novel KCNA1 mutations in episodic ataxia type I families. *Hum. Genet.* 102:464–466. http://dx.doi.org/10.1007/s004390050722

Seoh, S.A., D. Sigg, D.M. Papazian, and F. Bezanilla. 1996. Voltage-sensing residues in the S2 and S4 segments of the Shaker K^+ channel. *Neuron.* 16:1159–1167. http://dx.doi.org/10.1016/S0896-6273(00)80142-7

Shi, N., W. Zeng, S. Ye, Y. Li, and Y. Jiang. 2011. Crucial points within the pore as determinants of K^+ channel conductance and gating. *J. Mol. Biol.* 411:27–35. http://dx.doi.org/10.1016/j.jmb.2011.04.058

Simons, C., L.D. Rash, J. Crawford, L. Ma, B. Cristofori-Armstrong, D. Miller, K. Ru, G.J. Baillie, Y. Alanay, A. Jacquinet, et al. 2015. Mutations in the voltage-gated potassium channel gene *KCNH1* cause Temple-Baraitser syndrome and epilepsy. *Nat. Genet.* 47:73–77. http://dx.doi.org/10.1038/ng.3153

Singh, N.A., P. Westenskow, C. Charlier, C. Pappas, J. Leslie, J. Dillon, V.E. Anderson, M.C. Sanguinetti, and M.F. Leppert. BFNC Physician Consortium. 2003. *KCNQ2* and *KCNQ3* potassium channel genes in benign familial neonatal convulsions: expansion of the functional and mutation spectrum. *Brain.* 126:2726–2737. http://dx.doi.org/10.1093/brain/awg286

Starkus, J.G., L. Kuschel, M.D. Rayner, and S.H. Heinemann. 1997. Ion conduction through C-type inactivated Shaker channels. *J. Gen. Physiol.* 110:539–550. http://dx.doi.org/10.1085/jgp.110.5.539

Sukhareva, M., D.H. Hackos, and K.J. Swartz. 2003. Constitutive activation of the Shaker Kv channel. *J. Gen. Physiol.* 122:541–556. http://dx.doi.org/10.1085/jgp.200308905

Swenson, R.P. Jr., and C.M. Armstrong. 1981. K^+ channels close more slowly in the presence of external K^+ and Rb^+. *Nature.* 291:427–429. http://dx.doi.org/10.1038/291427a0

Syrbe, S., U.B. Hedrich, E. Riesch, T. Djémié, S. Müller, R.S. Møller, B. Maher, L. Hernandez-Hernandez, M. Synofzik, H.S. Caglayan, et al. EuroEPINOMICS RES. 2015. De novo loss- or gain-of-function mutations in KCNA2 cause epileptic encephalopathy. *Nat. Genet.* 47:393–399. http://dx.doi.org/10.1038/ng.3239

Tester, D.J., M.L. Will, C.M. Haglund, and M.J. Ackerman. 2005. Compendium of cardiac channel mutations in 541 consecutive unrelated patients referred for long QT syndrome genetic testing. *Heart Rhythm.* 2:507–517. http://dx.doi.org/10.1016/j.hrthm.2005.01.020

Thompson, J., and T. Begenisich. 2001. Affinity and location of an internal K^+ ion binding site in *Shaker* K channels. *J. Gen. Physiol.* 117:373–384. http://dx.doi.org/10.1085/jgp.117.5.373

Tombola, F., M.M. Pathak, P. Gorostiza, and E.Y. Isacoff. 2007. The twisted ion-permeation pathway of a resting voltage-sensing domain. *Nature.* 445:546–549. http://dx.doi.org/10.1038/nature05396

Treptow, W., and M. Tarek. 2006. Molecular restraints in the permeation pathway of ion channels. *Biophys. J.* 91:L26–L28. http://dx.doi.org/10.1529/biophysj.106.087437

Wang, W., S.S. Black, M.D. Edwards, S. Miller, E.L. Morrison, W. Bartlett, C. Dong, J.H. Naismith, and I.R. Booth. 2008. The structure of an open form of an *E. coli* mechanosensitive channel at 3.45 Å resolution. *Science.* 321:1179–1183. http://dx.doi.org/10.1126/science.1159262

Webster, S.M., D. Del Camino, J.P. Dekker, and G. Yellen. 2004. Intracellular gate opening in Shaker K^+ channels defined by high-affinity metal bridges. *Nature.* 428:864–868. http://dx.doi.org/10.1038/nature02468

Wilkens, C.M., and R.W. Aldrich. 2006. State-independent block of BK channels by an intracellular quaternary ammonium. *J. Gen. Physiol.* 128:347–364. http://dx.doi.org/10.1085/jgp.200609579

Wilson, M.A., C. Wei, P. Bjelkmar, B.A. Wallace, and A. Pohorille. 2011. Molecular dynamics simulation of the antiamoebin ion channel: linking structure and conductance. *Biophys. J.* 100:2394–2402. http://dx.doi.org/10.1016/j.bpj.2011.03.054

Xie, G., J. Harrison, S.J. Clapcote, Y. Huang, J.Y. Zhang, L.Y. Wang, and J.C. Roder. 2010. A new Kv1.2 channelopathy underlying cerebellar ataxia. *J. Biol. Chem.* 285:32160–32173. http://dx.doi.org/10.1074/jbc.M110.153676

Ye, S., Y. Li, and Y. Jiang. 2010. Novel insights into K^+ selectivity from high-resolution structures of an open K^+ channel pore. *Nat. Struct. Mol. Biol.* 17:1019–1023. http://dx.doi.org/10.1038/nsmb.1865

Yifrach, O., and R. MacKinnon. 2002. Energetics of pore opening in a voltage-gated K^+ channel. *Cell.* 111:231–239. http://dx.doi.org/10.1016/S0092-8674(02)01013-9

Yu, F.H., V. Yarov-Yarovoy, G.A. Gutman, and W.A. Catterall. 2005. Overview of molecular relationships in the voltage-gated ion channel superfamily. *Pharmacol. Rev.* 57:387–395. http://dx.doi.org/10.1124/pr.57.4.13

Yuan, P., M.D. Leonetti, Y. Hsiung, and R. MacKinnon. 2011. Open structure of the Ca^{2+} gating ring in the high-conductance Ca^{2+}-activated K^+ channel. *Nature.* 481:94–97. http://dx.doi.org/10.1038/nature10670

Zhang, Y., X. Niu, T.I. Brelidze, and K.L. Magleby. 2006. Ring of negative charge in BK channels facilitates block by intracellular Mg^{2+} and polyamines through electrostatics. *J. Gen. Physiol.* 128:185–202. http://dx.doi.org/10.1085/jgp.200609493

Zhou, Y., J.H. Morais-Cabral, A. Kaufman, and R. MacKinnon. 2001. Chemistry of ion coordination and hydration revealed by a K^+ channel–Fab complex at 2.0 Å resolution. *Nature.* 414:43–48. http://dx.doi.org/10.1038/35102009

Zhou, Y., X.M. Xia, and C.J. Lingle. 2011. Cysteine scanning and modification reveal major differences between BK channels and Kv channels in the inner pore region. *Proc. Natl. Acad. Sci. USA.* 108:12161–12166. http://dx.doi.org/10.1073/pnas.1104150108

Zhu, F., and G. Hummer. 2012a. Drying transition in the hydrophobic gate of the GLIC channel blocks ion conduction. *Biophys. J.* 103:219–227. http://dx.doi.org/10.1016/j.bpj.2012.06.003

Zhu, F., and G. Hummer. 2012b. Theory and simulation of ion conduction in the pentameric GLIC channel. *J. Chem. Theory Comput.* 8:3759–3768. http://dx.doi.org/10.1021/ct2009279